J. Geomag. Geoelectr., **47**, 1237–1247, 1995

Mesospheric Heating during Highly Relativistic Electron Precipitation Events

R. A. GOLDBERG, D. N. BAKER*, F. A. HERRERO, C. H. JACKMAN, S. KANEKAL**, and P. A. TWIGG**

NASA/Goddard Space Flight Center, Greenbelt, Maryland, U.S.A.

(Received November 28, 1994; Revised June 12, 1995; Accepted June 23, 1995)

Highly relativistic electron precipitation (HRE) events which occur in the mid-latitude and auroral regions last 2.5 days on the average, peaking in the magnetosphere daily near local noon. Furthermore, they can recur every 27 days for several synodic solar rotation periods, and become most intense and frequent during the minimum of the solar cycle. These events are described in terms of their spatial and temporal extent and their spectral characteristics. A detailed sounding rocket study of a relatively weak event in May, 1990 at Poker Flat, Alaska gave energy depositions from which modeling calculations have yielded O_3 depletion estimates in excess of 25% near 75 km altitude. These depletions would hardly affect the UV flux reaching the stratosphere below, but could alter the thermal balance in the 60–75 km altitude region in the mesosphere. Further analysis for that HRE has shown the possibility of Joule heating effects near the polar cusp of up to 3°/day depending on the magnitude of the electric field. The mesospheric heating caused by more intense events studied with SAMPEX (Solar Anomalous Magnetospheric Particle Explorer) is compared with the earlier May 1990 event to demonstrate the global impact of HRE events on the chemical and thermal characteristics of the neutral atmosphere.

1. Introduction

Highly relativistic electron events (HREs) provide the most intense and spectrally hard electron precipitation observed to date. Details of these events as observed at geosynchronous satellite altitudes can be found in Baker *et al.* (1979, 1986). From comparisons with lower altitude satellites (Imhof *et al.*, 1991), and from our rocket study of a weak-to-modest intensity HRE, it is apparent that a significant fraction of the outer zone (high altitude) electrons associated with an HRE reach the middle atmosphere (Herrero *et al.*, 1991; Baker *et al.*, 1993) and strongly influence the electrodynamics and chemical structure (e.g. OH and O_3) of that region (Goldberg *et al.*, 1994, 1995). Since HREs can sustain their activity for several days and recur over several solar rotations, and since they may cover a broader region in latitude than the auroral zone, their impact on the middle atmosphere is expected to be large. Based on satellite data, these events are most pronounced during the declining phase of the solar cycle, increasing in intensity, spectral hardness, and frequency of occurrence as the solar cycle reaches minimum (e.g., Baker *et al.*, 1987, 1993). Figure 1 provides a survey of such events measured by SAMPEX (Solar Anomalous Magnetospheric Particle Explorer) for about two years from launch in 1992. This spectogram representation shows the relativistic electron flux (>1 MeV) on a logarithmic color scale as a function of time and magnetic L value. The band of maxima observed near $L = 1.5$ corresponds to the inner radiation belts. The HREs that interest us correspond to the band of maxima occurring above $L = 2.5$. During this period of decline from solar maximum, the frequency of events is observed to increase. Furthermore, the latitudinal extent of precipitation during HREs can occasionally reach or exceed $L = 7$. Because such events can be sustained up to several days, their integrated effect on the high latitude mesosphere may dominate other energetic electron sources such as relativistic electron precipitation events (REPs), and possibly compete with solar proton events (SPEs). In May, 1990 we launched rockets from Poker Flat, Alaska during a weak-to-modest HRE to measure the characteristics of the radiation and its energy

*Now at the University of Colorado.

**Hughes STX Corporation

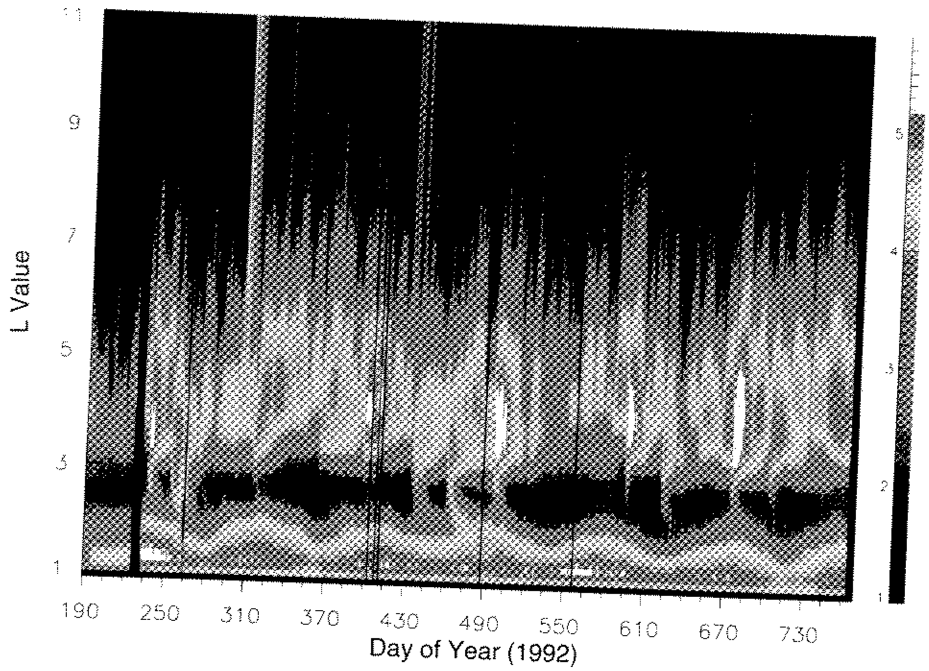

Fig. 1. Relativistic electron flux (>1 MeV) measured by the SAMPEX satellite as a function of time and magnetic L. The color code is a logarithmic representation of the flux.

deposition within the middle atmosphere. A description of these flights including the nature of the electron precipitation has already been reported in Herrero *et al.* (1991) and Baker *et al.* (1993). Effects on middle atmospheric electrodynamics (Goldberg *et al.*, 1994) and ozone (Goldberg *et al.*, 1995) have also been discussed. In this study, we concentrate on the impact that relativistic electron precipitation can have on mesospheric heating, making use of the rocket flight data and satellite comparisons.

2. Experiment Description and Data Analysis

The first Taurus Orion rocket payload was launched on May 13, 1990 at midday and reached an apogee in excess of 130 km. A second Taurus Orion payload was launched on the following day, also near noon. Each payload contained an x-ray scintillator and two solid state particle telescopes to measure precipitating energetic electron fluxes from 0.1 to 3.8 MeV. Details of the payload and instrument characteristics can be found in Herrero *et al.* (1991) and Goldberg *et al.* (1994). Figure 2 shows count rates from three representative channels on both the low energy (0.1–1 MeV) and high energy (0.5–3.8 MeV) electron telescope over the period of the flight. Also shown are the flight trajectory and payload pitch. Two of the three shaded regions refer to bursts 1 and 2, during which particles seemed to be injected at higher flux rates. Period 3 represents our estimate of the more nominal count rates during non-burst periods. The flux level for this period was similar in magnitude to that observed for the entire flight of 33.060 on the next day. The HRE measured by these rocket flights had a duration of about 4 days. The level of flux was considered to be weak-to-modest based on a comparison with satellite observations for events occurring in 1991–1993.

Figure 3 provides the energy deposition in terms of ion-pair production rate during both flights as reported in Goldberg *et al.* (1994, 1995). The four curves depict short burst periods "1" and "2" of intensity higher than non-burst period "3" on May 13, 1990 (NASA 33.059), and the steady value during the flight

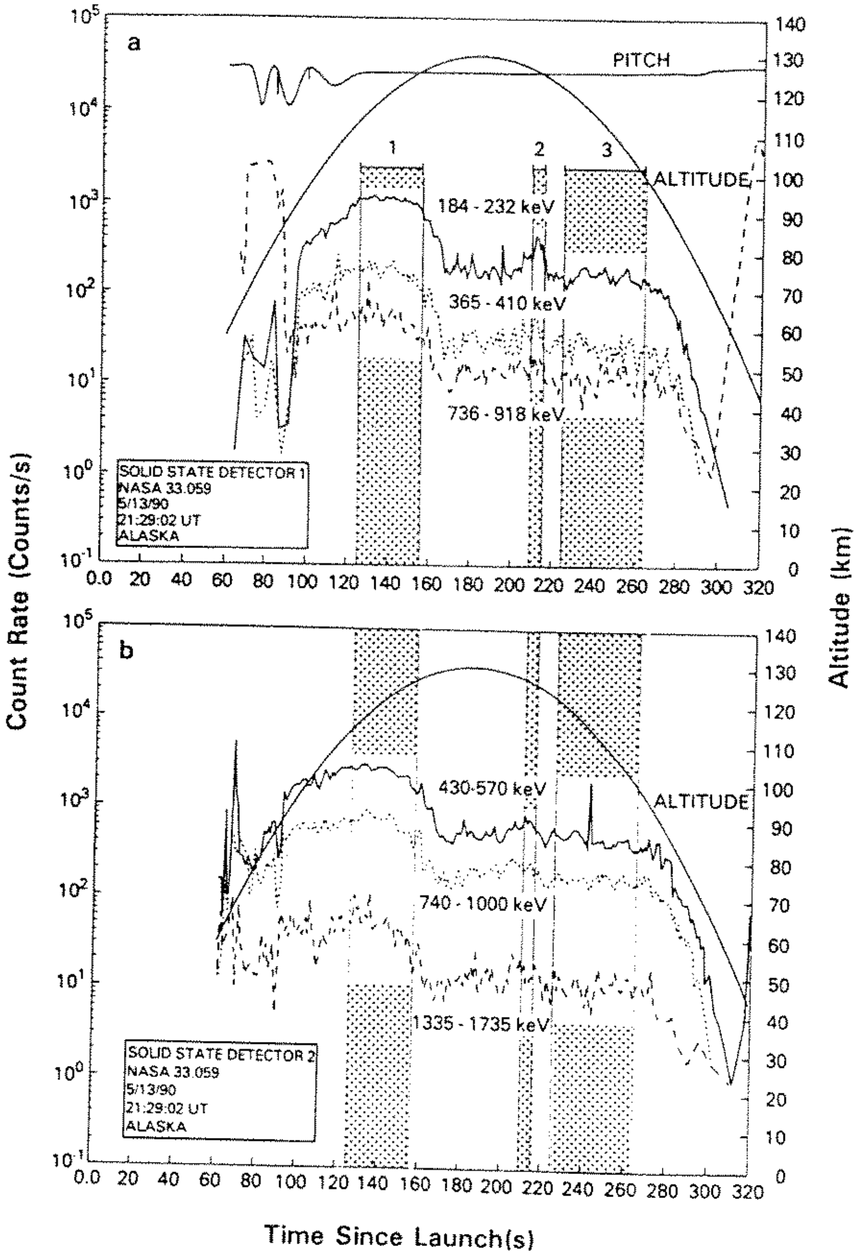

Fig. 2. Compressed view of counting rates (NASA 33.059) for three select channels on the low energy (top panel) and high energy (bottom panel) electron telescopes. Payload pitch attitude (arbitrary units) and trajectory are also provided.

on May 14, 1990 (NASA 33.060). These curves have been obtained from the electron energy spectrum using techniques described in Goldberg *et al.* (1984). Because of the 0.1 MeV instrument threshold for energetic electron measurements, we have restricted our results to altitudes below 80 km, where >0.1 MeV electrons normally penetrate with limited atmospheric absorption. The calculated cosmic ray background (Nicolet, 1975) is provided to demonstrate where this energy source dominates. No contribution from bremsstrahlung x-rays is provided since these were found to be negligible (Goldberg *et al.*, 1994, 1995).

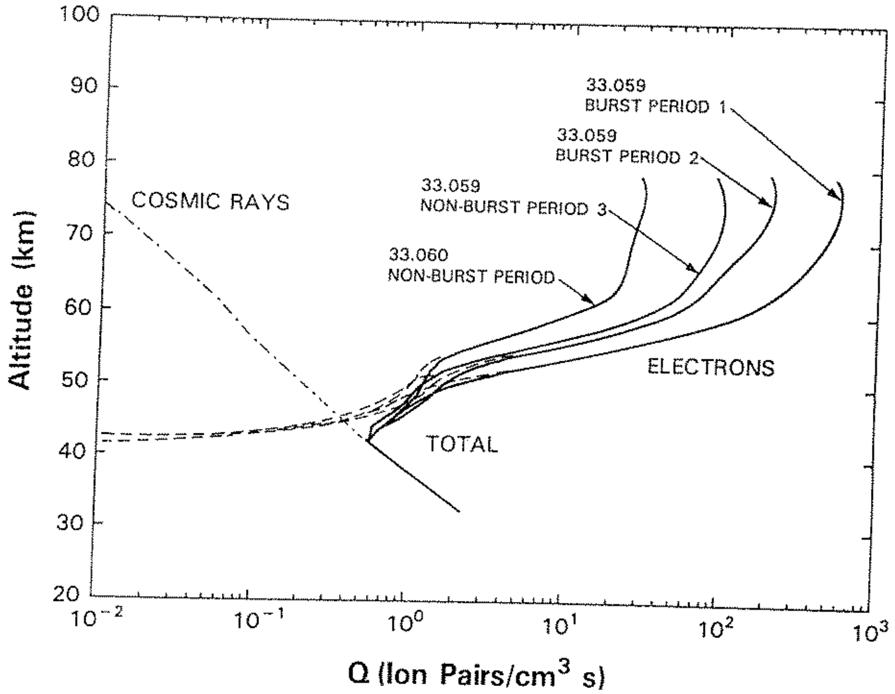

Fig. 3. Energy deposition profiles in terms of ion pair production rate caused by measured electrons. Shown are periods "1", "2", and "3" during the flight of 33.059 and the value during 33.060. Also included is the calculated effect from cosmic rays corrected for latitude and time of solar cycle. Maxima near 80 km are probably caused by limiting the electron spectrum to values above 100 keV, which is the low energy spectrometer threshold value.

Although this HRE event was of weak-to-modest intensity, it still managed to produce very large ion pair production rates in excess of any of our previously observed REP events associated with geomagnetic storms (e.g., Goldberg *et al.*, 1984, 1990). This was especially true during the burst periods.

3. Model Description and Results

Within the mesosphere, HO_x is the primary constituent affecting the loss of O_3 during particle precipitation events. HO_x enhancements can lead to O_3 depletions through several catalytic processes (e.g. Jackman and McPeters, 1987). O_3 depletions during SPEs have even been measured in the mesosphere (Weeks *et al.*, 1972; Thomas *et al.*, 1983; McPeters and Jackman, 1985). The O_3 depletions observed for the July 13, 1982 SPE were modeled from HO_x enhancements by Solomon *et al.* (1983). Depletions were measured by the SME satellite to be over 50% in the 70–82 km altitude region. Since energetic electrons interact with the atmosphere in much the same way as protons, it is believed that intense high-energy electron precipitation events could be associated with mesospheric O_3 depletion.

Our rocket measurements of electron fluxes during the May, 1990 HRE were compared with satellite measurements of electron fluxes sampled at 6.6 R_E and found to be much higher than expected, based on an isotropic pitch angle distribution at 6.6 R_E. The loss cone for electrons near the geomagnetic equator has a very small half-angle of roughly 2°. The electrons within this loss cone are those which precipitate to low altitudes, and a uniform distribution cannot account for the measured ratio of precipitated to equatorial electron fluxes, even with large measurement errors included (see Herrero *et al.*, 1991). Minor constituent changes from the energy deposition profiles shown in Fig. 3 were computed using a two-dimensional photochemical model (Jackman *et al.* 1990; Goldberg *et al.*, 1995). The 130 chemical reactions used are specified in the JPL 90-1 model (De More, 1990) with ground boundary conditions for the trace gases taken from WMO (1992). The residual circulation and diffusion specification is the Dynamics A formulation described in Jackman (1991). The maximum OH enhancement and associated O_3 decrease that would result from such an electron flux if it were assumed to be constant for five hours is shown in Fig. 4. The OH is computed to increase by about 40% between 70 and 80 km with commensurate O_3 decreases of over 25%.

The upper and lower panels of Fig. 4 display the vertical profiles for percentage change in OH and O_3 at the Poker Flat site during burst period "1" and non-burst period "3", assuming daytime average conditions for the date of the launch. These parameters have been calculated for the measured fluxes assuming a one day steady source. The model approaches the equilibrium value within a few hours. For a twilight condition, the maximum values for OH enhancement and O_3 depletion would change by a factor

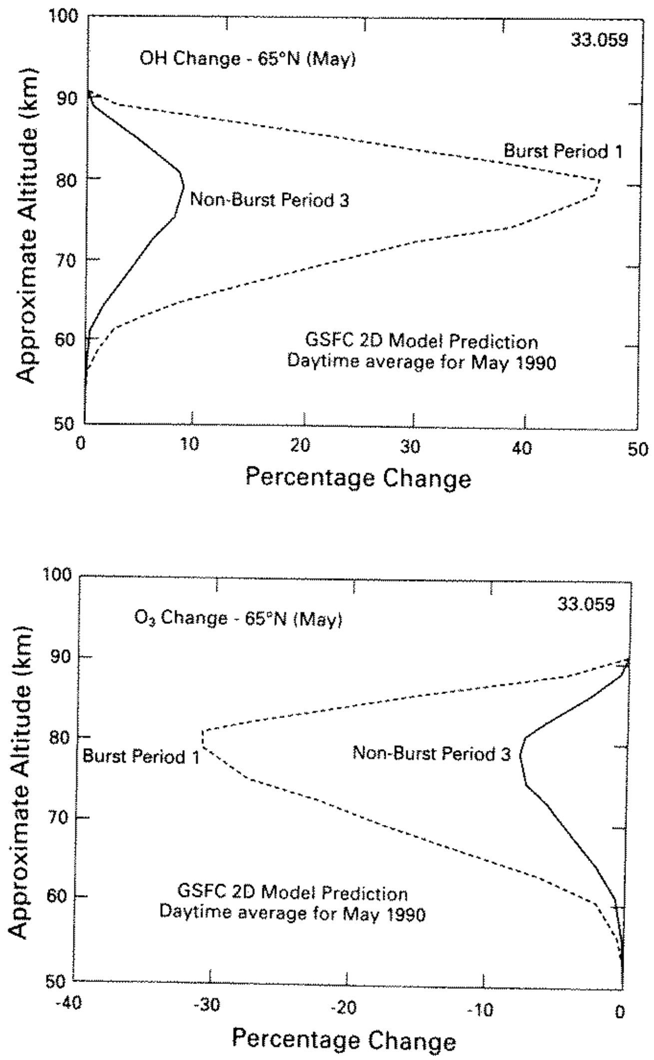

Fig. 4. The GSFC 2-D model prediction for the percent changes of the OH (upper panel) and O_3 (lower panel) mesospheric vertical profile at Poker Flat, Alaska (65°N) in May following bombardment by relativistic electrons with an intensity and spectral distribution equivalent to burst period "1" and non-burst period "3" in the measured HRE.

of 3 to 4. SAMPEX has recently measured several events exhibiting intensities of much larger magnitude as we approach solar minimum (Baker *et al.*, 1993). For an event ten times more intense than that measured by our rockets, we would expect O_3 to reach a maximum depletion of as much as 80% near 75 km, based on model calculations. For events showing similar fluxes with an enhanced hardness in the energy spectrum, this effect would penetrate more deeply into the atmosphere.

4. Heating Effects

London (1980) reviewed the radiative effects induced by absorption of solar UV in the mesosphere. He showed that radiative heating by O_3 and cooling by CO_2 each reach a maximum magnitude of about 12°K/day but nearly balance at 50 km (Fig. 5A), leading to a small net heating effect which nearly cancels out at all altitudes up to 90 km (Fig. 5B). From his results, it is apparent that O_3 depletions of the magnitudes discussed above would create a major imbalance, reducing the heating approximately linearly with the O_3 depletion, thereby resulting in an effective radiative cooling of the region. From Fig. 5, it appears that a 25–30% depletion could reduce mesospheric heating near 75 km by several °K/day. For more intense HRE events, the O_3 depletions would be somewhat larger, thereby enhancing this effect.

Joule heating (Cole, 1963) by electrons must also be considered as a potential heating source in this region of the mesosphere since the Pedersen conductivity (σ_P) is enhanced by the HRE down to 65 km. Joule heating is given by

$$Q_J = \sigma_P E^2 = \frac{7}{2} Nk \frac{dT}{dt} \tag{1}$$

where E is the electric field, N is atmospheric concentration, k is Boltzman's constant and T is temperature. The electron density (n_e) can be determined from the ion-pair production rates (P) given in Fig. 3 assuming knowledge of the effective recombination coefficient (α_R) from

$$n_e = \sqrt{\frac{P}{\alpha_R}}. \tag{2}$$

σ_P can then be determined from Eq. (3)

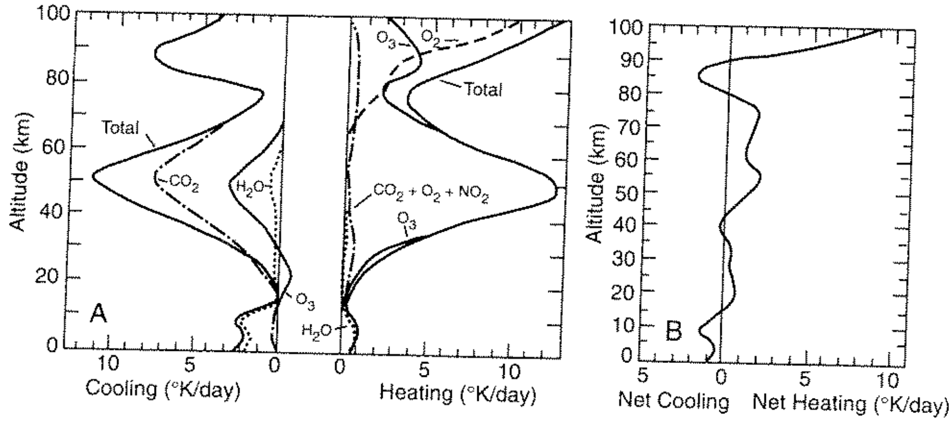

Fig. 5. Vertical distribution of solar short wave heating rates by O_3, O_2, NO_2, H_2O, CO_2, and of terrestrial long wave cooling rates by CO_2, O_3, and H_2O (panel A) and the resulting net radiative heating/cooling (panel B) (from London, 1980).

$$\sigma_P = \frac{en_e}{B}\frac{\nu\omega}{\nu^2+\omega^2} \tag{3}$$

where B is the magnetic field, e is the electronic charge, and ν and ω are electron collision and gyro frequencies respectively. Within the region of interest, ~65–80 km, $\nu \cong \omega$, so that $\nu\omega/(\nu^2+\omega^2) \cong 1/2$. Figure 6 shows the ion pair production rate and calculated ion density profiles (Eq. (2)) used for this analysis for the burst "1" period. A nominal value of 1×10^{-7} cm^3 s^{-1} was used for the ion-ion recombination coefficient in this altitude region. Figure 7 exhibits the resulting σ_P profile, which is found to maximize near 70 km altitude with a value of about 9×10^{-5} Siemens/m.

Our final step requires estimation of the mesospheric electric field. Figure 8 (after Roble *et al.*, 1987) provides the electric field measured by the Dynamics Explorer (DE-2) satellite for high latitude in the northern hemisphere on July 13, 1982 during a solar proton event. This demonstrates that the electric field can reach values as high as 200 mV/m near the polar magnetic cusp region during precipitating particle events. In this case, the maximum electric field was at 72.2° geomagnetic latitude with a gradual decline north of the peak. The model of Heppner and Maynard (1987) indicates that the highest fields should appear in this region during local afternoon, which is within the diurnal period of maximum HRE flux. Figure 9 displays a polar plot example of their estimated convection electric field, empirically modeled assuming modest magnetic activity. We would expect such fields to map down to mesospheric altitudes without great difficulty. Finally, SAMPEX data (cf. Fig. 1) show that HREs can reach or overlap this region, implying that at such times, the high energy electron stream could interact with electric fields of this magnitude.

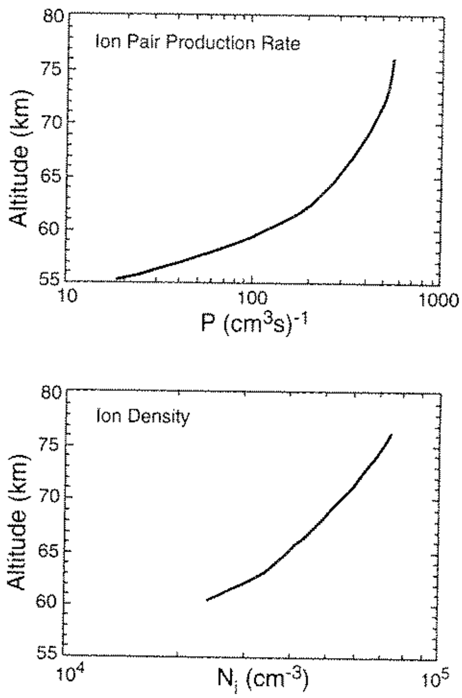

Fig. 6.

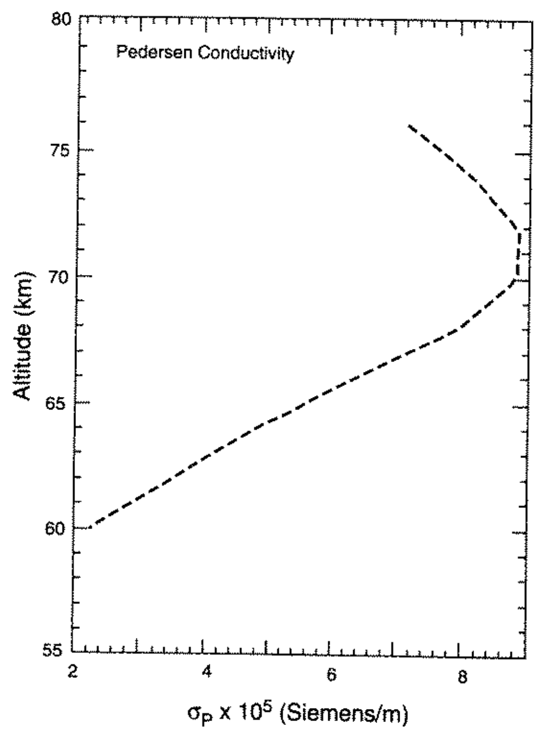

Fig. 7.

Fig. 6. Vertical height profiles for P (top) and N_i (bottom) using the burst "1" curve in Fig. 3.

Fig. 7. Calculated vertical height profile for Pedersen conductivity during burst "1" of rocket flight 33.059.

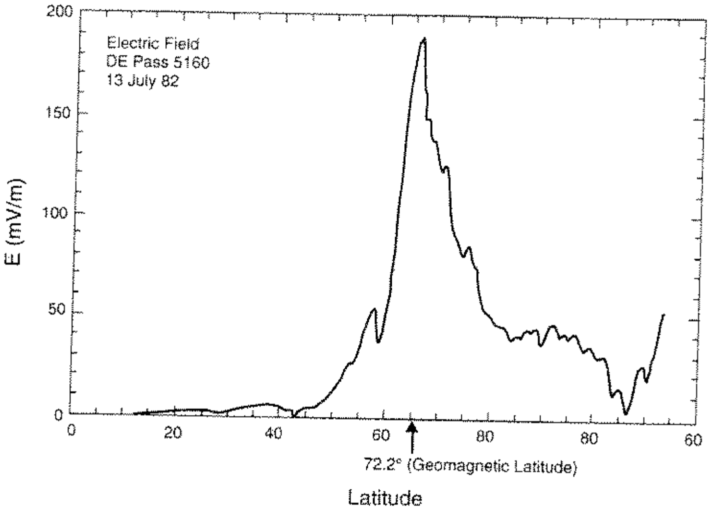

Fig. 8. Electric field magnitude (mV/m) as a function of latitude as measured by the DE-2 satellite on July 13, 1982 (after Roble *et al.*, 1987).

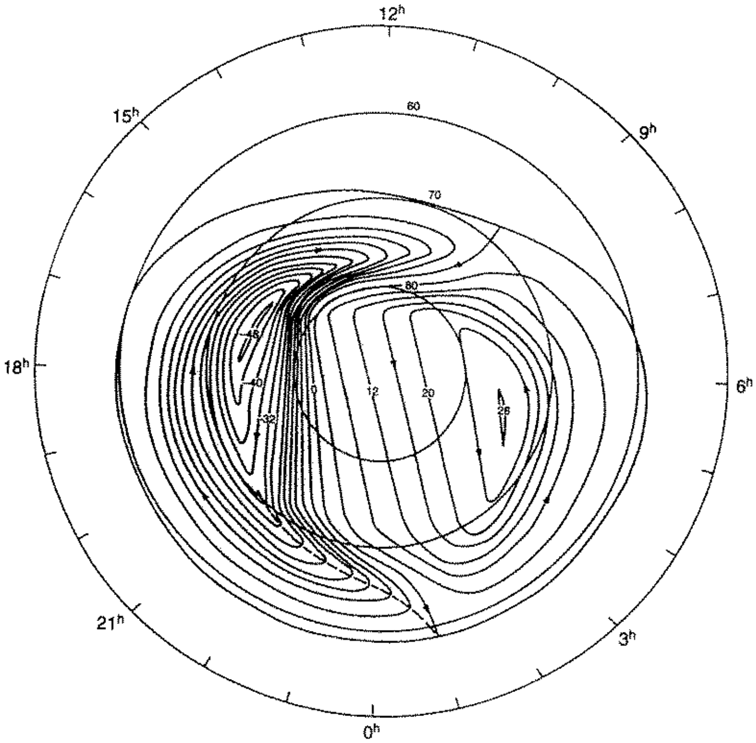

Fig. 9. Empirical model of the convective electric field in the northern hemisphere under modestly active magnetic conditions (from Heppner and Maynard, 1987). The contour lines represent E in mV/m.

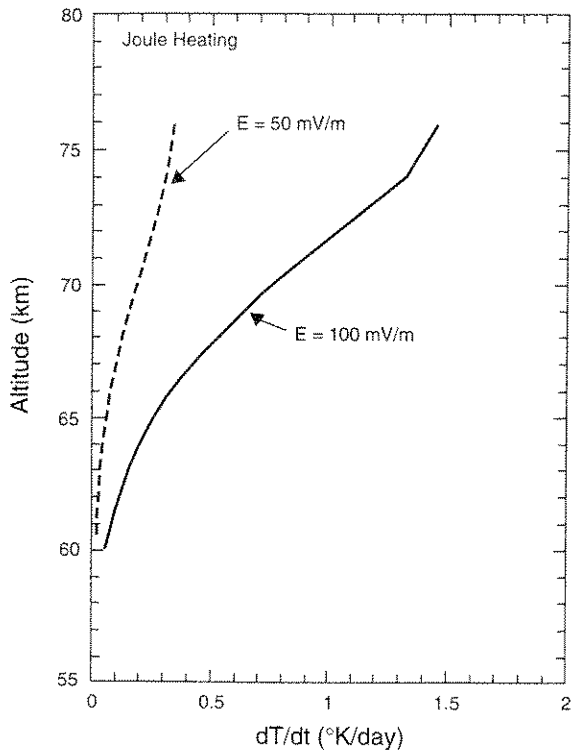

Fig. 10. Joule heating rates during burst "l" assuming values of E at 50 and 100 mV/m.

Figure 10 shows the expected Joule heating rates for typical electric fields of 50 and 100 mV/m during solar and/or magnetically active events, using the values for P, N_i, and σ_P, as determined from Eqs. (1)–(3) and shown in Figs. 6 and 7. For more unusual electric field magnitudes approaching 200 mV/m, the 100 mV/m heating rates should increase by a factor of 4 to values near 3°K/day, making this heating source competitive with the ozone absorption heating rates. Here, Joule heating is most sensitive to the magnitude of the electric field, being proportional to E^2 (cf Eq. (1)). Furthermore, since ozone depletion effects would probably maximize at a different altitude than the Joule heating maximum, reducing ozone by electron precipitation could induce stronger vertical temperature gradients throughout the region than normal, thereby perturbing the local dynamics similar to those changes reported by the Johnson and Luhmann (1993) study of MST radar data at Poker Flat, Alaska during solar proton events. Finally, for more intense HRE events than the weak-to-modest one measured by our rockets, we would expect the heating rate to increase proportionally with the enhanced electron density, which in turn is proportional to $P^{1/2}$ (cf. Eqs. (1)–(3)). Thus, it appears that Joule heating rates may compete with radiative heating effects caused by the destruction of O_3, but only in localized regions.

5. Conclusions

From rocket data obtained in Alaska during May, 1994 during a relatively modest HRE, we have calculated that ozone depletion by HREs could reduce ozone by 25% or more in the mesosphere, reducing its absorption of solar UV and effectively reducing heating of this region by several °K/day. The same event may have caused Joule heating in the mesosphere, which for equivalent numbers and an electric field of 200 mV/m, could heat that region by several °K/day. Since the atmospheric absorption of UV and Joule heating do not maximize at the same altitude, we suggest that vertical temperature gradients would be enhanced, affecting the dynamics of the region. In fact, Johnson and Luhmann (1993) have reported significant dynamical effects in the mesosphere during solar proton events, from a study of MST data at Poker Flat, Alaska, although these effects could have been caused by induced horizontal temperature gradients as well.

We note that the strong perturbation of solar UV heating would be limited to daylight hours, but could be quite extensive over the entire region of electron precipitation. Important Joule heating on the other hand, would be limited to localized regions and times where and/or when the electric field could reach values in excess of about 100 mV/m. In general, since the reduction in UV heating and the enhancement in Joule heating do not necessarily occur at the same altitude, more intense HREs could enhance vertical and horizontal temperature gradients and the ensuing dynamics.

REFERENCES

Baker, D. N., P. R. Higbie, R. D. Belian, and E. W. Hones, Jr., Do Jovian electrons influence the terrestrial outer radiation zone?, *Geophys. Res. Lett.*, **6**, 531–534, 1979.

Baker, D. N., J. B. Blake, R. W. Klebesadel, and P. R. Higbie, Highly relativistic electrons in the Earth's outer magnetosphere. 1; Lifetimes and temporal history, 1979–1984, *J. Geophys. Res.*, **91**, 4265–4268, 1986.

Baker, D. N., J. B. Blake, D. J. Gorney, P. R. Higbie, R. W. Klebesadel, and J. H. King, Highly relativistic electrons: A role in coupling to the middle atmosphere, *Geophys. Res. Lett.*, **14**, 1027–1030, 1987.

Baker, D. N., R. A. Goldberg, F. A. Herrero, J. B. Blake, and L. B. Callis, Satellite and rocket studies of relativistic electrons and their influence on the middle atmosphere, *J. Atmos. Terr. Phys.*, **54**, 1619–1628, 1993.

Cole, K. D., Joule heating of the ionosphere over Halley Bay, *Nature*, **199**, 444–445, 1963.

De More, W. B., S. P. Sander, D. M. Golden, M. J. Molina, R. F. Hampson, M. J. Kurylo, C. J. Howard, and A. R. Ravishankara, Chemical kinetics and photochemical data for use in stratospheric modeling, *JPL Publication 90-1*, 217 pp., 1990.

Goldberg, R. A., C. H. Jackman, J. R. Barcus, and F. Sørass, Nighttime auroral energy deposition in the middle atmosphere, *J. Geophys. Res.*, **89**, 5581–5596, 1984.

Goldberg, R. A., C. L. Croskey, L. C. Hale, J. D. Mitchell, and J. R. Barcus, Electrodynamic response of the middle atmosphere to auroral pulsations, *J. Atmos. Terr. Phys.*, **52**, 1067–1084, 1990.

Goldberg, R. A., D. N. Baker, F. A. Herrero, S. P. McCarthy, P. A. Twigg, C. L. Croskey, and L. C. Hale, Energy deposition and middle atmosphere electrodynamic response to a highly relativistic electron precipitation event, *J. Geophys. Res.*, **99**, 21071–21081, 1994.

Goldberg, R. A., C. H. Jackman, D. N. Baker, and F. A. Herrero, Changes in the concentration of mesospheric O_3 and OH during a highly relativistic electron precipitation event, in *The Upper Mesosphere and Lower Thermosphere: A Review of Experiment and Theory*, edited by R. M. Johnson and T. L. Killeen, pp. 215–224, American Geophysical Union: Geophysical Monograph 87, Washington, D.C., 1995.

Heppner, J. P. and N. C. Maynard, Empirical high-latitude electric field models, *J. Geophys. Res.*, **92**, 4467–4489, 1987.

Herrero, F. A., D. N. Baker, and R. A. Goldberg, Rocket measurements of relativistic electrons: New features in fluxes, spectra, and pitch angle distributions, *Geophys. Res. Lett.*, **18**, 1481–1484, 1991.

Imhof, W. L., H. D. Voss, J. Mobilia, D. W. Datlowe, J. P. McGlennon, and D. N. Baker, Relativistic electron enhancement events: Simultaneous measurements from synchronous and low altitude satellites, *Geophys. Res. Lett.*, **18**, 397–400, 1991.

Jackman, C. H. and R. D. McPeters, Solar proton events as tests for the fidelity of middle atmospheric models, *Physica Scripta*, **T18**, 309–316, 1987.

Jackman, C. H., A. R. Douglass, R. B. Rood, R. D. McPeters, and P. E. Meade, Effect of solar proton events on the middle atmosphere during the past two solar cycles as computed using a 2-dimensional model, *J. Geophys. Res.*, **95**, 7417–7428, 1990.

Jackman, C. H., Effects of energetic particles on minor constituents of the middle atmosphere, *J. Geomag. Geoelectr.*, **43**, 637–646, 1991.

Johnson, R. M. and J. G. Luhmann, Poker Flat MST radar observations of high latitude neutral winds at the mesopause during and after solar proton events, *J. Atmos. Terr. Phys.*, **55**, 1203–1218, 1993.

London, J., Radiative sources and sinks in the stratosphere and mesosphere, in *Proceedings of the NATO Advanced Study Institute on Atmospheric Ozone* (Portugal), p. 703–720, U.S. Dept. of Transportation, FAA, Washington, D.C., #FAA-EE-80-20, 1980.

McPeters, R. D. and C. H. Jackman, The response of ozone to solar proton events during solar cycle 21: The observations, *J. Geophys. Res.*, **90**, 7945–7954, 1985.

Nicolet, M., On the production of nitric oxide by cosmic rays in the mesosphere and stratosphere, *Planet. Space Sci.*, **23**, 637–649, 1975.

Roble, R. G., B. A. Emry, T. L. Killeen, G. C. Reid, S. Solomon, R. R. Garcia, D. S. Evans, P. B. Hays, G. R. Carignan, R. A. Heelis, W. B. Hanson, D. J. Winningham, N. W. Spencer, and L. H. Brace, Joule heating in the mesosphere and thermosphere during the July 13, 1982, solar proton event, *J. Geophys. Res.*, **92**, 6083–6090, 1987.

Solomon, S., G. C. Reid, D. W. Rusch, and R. J. Thomas, Mesospheric ozone depletion during the solar proton event of July 13, 1982; Part II. Comparison between theory and measurements, *Geophys. Res. Lett.*, **10**, 257–260, 1983.

Thomas, R. J., C. A. Barth, G. J. Rottman, D. W. Rusch, G. H. Mount, G. M. Lawrence, R. W. Sanders, G. E. Thomas, and L. E. Clemens, Mesospheric ozone depletion during the solar proton event of July 13, 1982, Part I, Measurement, *Geophys. Res. Lett.*, **10**, 253–255, 1983.

Weeks, L. H., R. S. CuiKay, and J. R. Corbin, Ozone measurements in the mesosphere during the solar proton event of November 2, 1969, *J. Atmos. Sci.*, **29**, 1138–1142, 1972.

WMO, Scientific assessment of ozone depletion: 1991, World Meteorological Organization, Global Ozone Research and Monitoring Project, *Report No. 25*, edited by D. L. Albritton, R. T. Watson, S. Solomon, R. F. Hampson, and F. Ormand, 1992.